ChemComm

COMMUNICATION

View Article Online
View Journal | View Issue

Cite this: *Chem. Commun.*, 2014, **50**, 10622

Received 17th May 2014,
Accepted 18th July 2014

DOI: 10.1039/c4cc03774j

www.rsc.org/chemcomm

Exfoliated layered copper phosphonate showing enhanced adsorption capability towards Pb ions†

Wei-Xuan Nie, Song-Song Bao, Dai Zeng, Li-Rong Guo‡ and Li-Min Zheng*

Copper 5-(2-bromothienyl)phosphonate (1) with a layered structure is obtained *via* solvothermal reaction. The layers can be successfully exfoliated using a "top-down" approach, resulting in 2D nanosheets. The exfoliated sample shows an enhanced adsorption capability to the Pb(II) ions in aqueous solution compared with that of the bulk material.

Since the report of graphene, the atomically thick two-dimensional (2D) nanosheets have been of great current interest as they are widely regarded as prototype materials for ultrathin nano-devices with novel features quite different from their bulk counterparts.[1] Many kinds of 2D nanosheets have been reported, most of which are purely inorganic or organic materials such as metal oxides,[2] metal hydroxides,[3] metal chalcogenides,[4] organic polymers[5] and so on.[6] However, 2D nanosheets concerned with inorganic–organic hybrid materials still remain rare. Two approaches are commonly used to obtain inorganic–organic hybrid nanosheets: (1) a "bottom-up" route to assemble inorganic nanosheets and organic components alternately through a layer-by-layer technique[7] or connect the inorganic and organic parts into 2D hybrid nanosheets;[8] (2) a "top-down" approach to exfoliate bulk inorganic–organic hybrid materials, featuring covalently bonded layer structures with merely weak inter-layer interactions, into nanosheets.[9] Due to the lack of intrinsic driving force for 2D anisotropic growth, it is often difficult to control the assembly of inorganic and organic components using the "bottom-up" method. In contrast, the "top-down" method *via* exfoliation would be a cost-effective and readily available approach to produce inorganic–organic hybrid nanosheets from the corresponding layered materials.[10]

State Key Laboratory of Coordination Chemistry, School of Chemistry and Chemical Engineering, Nanjing University, Nanjing 210093, P. R. China.
E-mail: lmzheng@nju.edu.cn

† Electronic supplementary information (ESI) available: Crystal data in CIF file; selected bond lengths and angles, PXRD, TG curves, IR spectra, AFM and SEM images. CCDC 998012. For ESI and crystallographic data in CIF or other electronic format see DOI: 10.1039/c4cc03774j

‡ Current address: College of Chemistry and Chemical Engineering and State Key Laboratory of Applied Organic Chemistry, Lanzhou University, Lanzhou 730000, P. R. China.

As an important class of inorganic–organic hybrid materials, metal phosphonates have received increasing attention during the past two decades owing to their potential applications in ion-exchange and sorption,[11] catalysis,[12] proton conductivity[13] and magnetism,[14] *etc.* Most of the reported metal phosphonates display layered structures, hence providing the potential to be exfoliated into nanosheets due to the weak inter-layer interactions. Furthermore, the organic groups of the phosphonate ligands can be designed and modified for specific purpose. However, as far as we are aware, there is only one report in the literature on the exfoliation of metal phosphonates, *e.g.* lanthanum 1,3,5-benzenetriphosphonate.[15] The photoluminescence of both the bulk and exfoliated samples has been studied.

In this communication, we report the first example of metal phosphonates based on 5-(2-bromothienyl)phosphonic acid ($BrC_4H_2SPO_3H_2$, 2-BTPH$_2$), namely, [Cu(H_2O)(2-BTP)] (**1**). The 2-BTP^{2-} ligand has been chosen because of its potential affinity for the adsorption of toxic heavy metal ions such as Pb(II) through the uncoordinated Br and S atoms. Compound **1** shows a layer structure. The layers can be successfully exfoliated into nanosheets through ultrasonic treatment. As far as we are aware, compound **1** provides the first example of metal phosphonates that exhibit enhanced adsorption capability towards Pb(II) ions due to exfoliation.

Blue-green crystals of **1** were obtained by solvothermal reaction of Cu(NO_3)$_2$·3H_2O and 2-BTPH$_2$ (molar ratio 1 : 1) in a mixed solvent of methanol and water (4.0/2.5, v/v) at 120 °C for 2 days.§ The ratio of the mixed solvents is quite critical for the formation of the layer structure of **1**. The reduction of water content (methanol/water: 5/1.5, v/v) in the reaction mixture leads to the isolation of another phase of anhydrous compound [Cu(2-BTP)] (**2**).[16] Compounds **1** and **2** can be converted to each other *via* dehydration and rehydration processes in a reversible manner (Fig. S5, ESI†). Single crystal structural analysis reveals that compound **1** crystallizes in the monoclinic lattice with the $P2_1/c$ space group. As shown in Fig. 1, the asymmetric unit consists of one Cu(II) ion, one 2-BTP^{2-} and one coordinated water. The Cu atom exhibits a distorted square pyramidal geometry. The four basal sites are occupied by oxygen atoms of three equivalent phosphonate

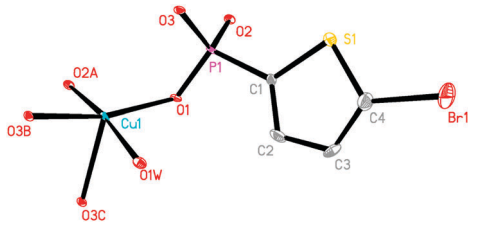

Fig. 1 Building unit of **1** with an atomic labeling scheme (30% probability). All hydrogen atoms are omitted for clarity.

groups (O1, O2A, O3B) and one water (O1W) [Cu–O: 1.919(4)–1.991(5) Å]. The apical position is occupied by O3C of another equivalent phosphonate group with a longer bond length [Cu1–O3C: 2.314(4) Å] due to the Jahn–Teller effect. In turn, each 2-BTP^{2-} ligand binds to four copper atoms through its three phosphonate oxygen atoms. One of them (O3) serves as μ_3-O bridging two equivalent copper atoms into a dimer. The Cu1···Cu1 distance over the μ_3-O3 bridge is 3.090 Å. The Cu1–O3–Cu1 angle is 92.25°. The $\{Cu_2O_2\}$ dimers are connected by the phosphonate groups through vertex-sharing of $\{PO_3C\}$ tetrahedra and $\{CuO_5\}$ square-pyramids, leading to a two-dimensional layer in the *bc* plane (Fig. 2a). The 2-bromothienyl groups are grafted onto both sides of the layer. Weak hydrogen bond interactions are found between the organic groups within the layer [C2···S1^{i} 4.876(7) Å, ∠C2–H···S1^{i} 153.7(4)°; C3···Br1^{i} 4.773(9) Å, ∠C3–H···Br1^{i} 143.4(5)°. Symmetry code: (i), *x*, 0.5 − *y*, 0.5 + *z*]. The layers are packed along the *a*-axis by van der Waals attractions between the organic groups (Fig. 2b). The shortest Br···Br contact between the layers is 4.184(2) Å.

The magnetic properties of compound **1** are studied. As shown in Fig. S6 (ESI†), the effective moment per Cu at 300 K (1.91 μ_B) is close to the theoretical value of 1.82 μ_B for an isolated spin S = 1/2 with g = 2.1. Upon cooling, χ_M increases continuously until reaching a maximum of 0.058 cm^3 mol^{-1} at 3.6 K, below which the χ_M value drops. The appearance of the peak in the χ_M *vs.* T plot and the monotonous decrease of $\chi_M T$ upon cooling confirm the dominant antiferromagnetic exchange couplings between the Cu(II) centers. Considering that the layer structure of **1** is made up of $\{Cu_2O_2\}$ dimers inter-linked by O–P–O bridges, the magnetic data can be analyzed by the Bleaney–Bowers expression.[17] The best fit in the whole temperature range leads to parameters g = 2.22, $2J$ = −4.6 cm^{-1}, ρ = 5.02% and zJ' = 0.15 cm^{-1}, where $2J$ is the exchange coupling constant within the Cu_2O_2 dimer, zJ' accounts for the interaction between the dimers, and ρ is the paramagnetic impurity. The $2J$ value is comparable with those in $Cu(C_6H_{10}(OH)PO_3)$ (J = −3.05 cm^{-1}) and $Cu(C_6H_9PO_3)(H_2O)$ (J = −2.73 cm^{-1}) containing similar layer structures.[18]

Since the inter-layer interaction in compound **1** is weak, it is possible to exfoliate the layers *via* a conventional "top-down" approach. Thus, the bulk sample of **1** (1 mg) suspended in an aqueous solution (5 mL) was subjected to ultrasonic treatment (300 W) for 2 hours at room temperature. The resulting mixture was left undisturbed in air for 24 hours. As shown in Fig. 3b, the Tyndall effect is clearly observed in the supernatant. The colloidal character of the suspension could originate from the finely dispersed nanosheets of the exfoliated compound **1**. To further confirm the formation of nanosheets, the suspension was also examined by atom force microscopy (AFM). Hence the droplets (5 μL) of the supernatant were dropped onto the freshly cleaved mica substrate and then the solvent was volatilized under the infrared light. The AFM images show clearly the presence of the nanosheets with a lateral dimension of 0.2–0.5 μm and an almost uniform thickness of 3.2–3.4 nm. The latter is comparable to the thickness of a two-layer overlapped stack (3.12 nm) estimated from the single crystal data. In other words, the bulk crystal sample could be successfully exfoliated into nanosheets with two-layer thickness.

Scanning electron microscope (SEM) measurements were also carried out for both the supernatant and the precipitate of the ultrasonicated sample of **1**. The nanosheets dispersed in the supernatant could not be clearly observed by SEM. However, the SEM images of the precipitates show the stacking of the nanosheets which are not fully exfoliated (Fig. 3d). The colloidal solution was then centrifuged and the precipitate of nanosheets was collected, the PXRD pattern of which matches well with that of the as-made bulk crystalline sample of compound **1** (Fig. S7, ESI†). The results indicate that the structure of **1** is maintained in colloidal solution after the exfoliation process.

As described above, compound **1** has a layer structure with the 2-bromothienyl groups filling in the inter-layer space. The uncoordinated Br and S atoms can potentially bind the heavy metal ions such as Pb(II). The exfoliation of **1** can lead to the exposure of more 2-bromothienyl groups for coordination with metal ions. Hence the adsorption capability of the exfoliated sample is expected to be enhanced compared with the crystalline

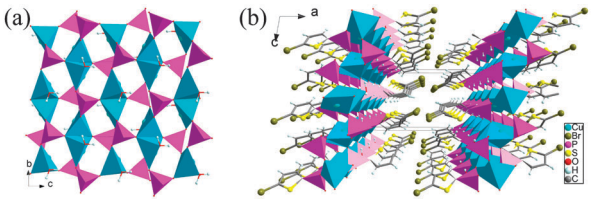

Fig. 2 (a) Inorganic layer of **1** viewed along the *a*-axis. (b) Packing diagram of **1** viewed along the *b*-axis.

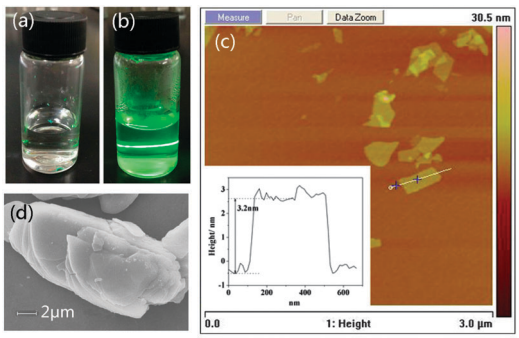

Fig. 3 The Tyndall effect of the supernatant in solvent water before ultrasonication (a) and after ultrasonication (b). (c) AFM images and the corresponding thickness of nano-sheets of **1**. (d) SEM image of the precipitate after ultrasonication.

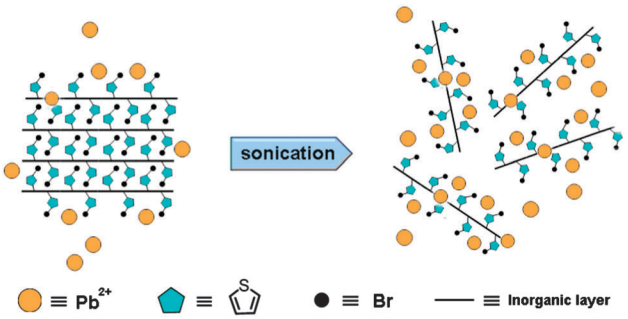

Scheme 1 Enhanced adsorption capability of the exfoliated sample.

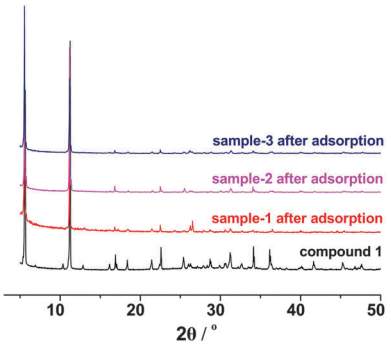

Fig. 4 The PXRD patterns of samples after adsorption and the as-synthesized bulk crystalline sample of compound **1**.

bulk sample (Scheme 1). In order to check our expectation, the adsorption experiments for Pb(II) ions have been designed and performed using three different methods. The details are listed in Table 1.

In method-1, we merely immersed the crystalline sample of **1** in 10 mL of 0.1 M $Pb(NO_3)_2$ solution for 24 hours. In method-2, a mixture of crystalline sample **1** in 10 mL of 0.1 M $Pb(NO_3)_2$ solution was first mechanically stirred for 2 hours and then allowed to stand for 22 hours. In method-3, a mixture of crystalline sample **1** in 10 mL of 0.1 M $Pb(NO_3)_2$ solution was first ultrasonicated for 2 hours and then allowed to stand for 22 hours. Afterwards, all three samples were centrifuged and washed by water three times. The PXRD patterns of the resulting samples agree well with that of the bulk crystalline sample of **1** (Fig. 4), indicating that no significant structural change occurs during the adsorption. The conclusion is also supported by IR spectra (Fig. S10, ESI†).

The Inductively Coupled Plasma (ICP) technique was employed to figure out the c(Pb)/c(Cu) ratio in the three samples. As shown in Table 1, the c(Pb)/c(Cu) ratio in sample-2 after adsorption is about twice that in sample-1. While the c(Pb)/c(Cu) ratio in sample-3 after adsorption is increased by about 1 order of magnitude compared with that in sample-1. The significant enhancement of the absorption capability in sample-3 is attributed to the efficient exfoliation of compound **1** under sonication conditions.

In order to check the stability of compound **1** in water and the possible metal replacement, the ICP measurements are also carried out for the solution of compound **1** after treatments by method-1, -2 and -3. The results are given in Table S3 (ESI†). Compared with the dissolution of the crystalline sample of **1** in pure water, the dissolution in 0.1 M $Pb(NO_3)_2$ increases slightly in the cases of method-1 (0.88% *vs.* 0.65% in water) and method-3 (3.43% *vs.* 2.25% in water), but decreases slightly in the case of method-2 (1.66% *vs.* 1.84% in water). Considering the possible error during the ICP measurements, the amount of replacement of Cu(II) by Pb(II) ions within the layer should be small. Assuming that the extra dissolution of Cu(II) in 0.1 M $Pb(NO_3)_2$ is due to the replacement of Cu(II) by Pb(II) in the solid material, we can calculate the expected c(Pb)/c(Cu) ratio in the solid sample, as shown in Table S3 (ESI†). Indeed, the experimental c(Pb)/c(Cu) ratio in the solid sample using method-1 (1.89×10^{-3}) is quite close to that expected for the sample due to the metal-replacement (2.23×10^{-3}). For method-3, however, the experimental c(Pb)/c(Cu) ratio (17.7×10^{-3}) is about 1.6 times of that expected for the sample due to the metal-replacement (11.3×10^{-3}). Thus the exfoliation of compound **1** under ultrasonic conditions could enhance the adsorption of Pb(II) ions through both the metal-replacement and the exposed organic ligands of the nanosheets (Scheme 1).

To further determine whether the organic ligand plays an important role in the adsorption of Pb(II) ions, similar experiments are conducted using a related layer compound $[Cu(H_2O)(O_3PC_6H_5)]$ in which the phenyl groups fill in the interlayer spaces.[20] As shown in Table S4 (ESI†), although this compound seems to be more stable in pure water than compound **1**, a significant increase of dissolution is observed in 0.1 M $Pb(NO_3)_2$ (*ca.* 2–3 times that of **1**). The fact that compound **1** is much more stable in 0.1 M $Pb(NO_3)_2$ than $[Cu(H_2O)(O_3PC_6H_5)]$ could be explained by the stronger intralayer and interlayer interactions in the former case through C–H···S, C–H···Br and Br···Br contacts. Hence, it is important to design particular phosphonate ligands in order to increase the stability of the corresponding metal phosphonates in an aqueous solution of $Pb(NO_3)_2$.

It is interesting to note that the c(Pb)/c(Cu) ratios in the solid samples of $[Cu(H_2O)(O_3PC_6H_5)]$ after adsorption treatments are about one order of magnitude less than the expected values assuming that the extra dissolution of Cu(II) in 0.1 M $Pb(NO_3)_2$ is due to the replacement of Cu(II) by Pb(II) in the solid materials. Obviously, an appreciable amount of $[Cu(H_2O)(O_3PC_6H_5)]$ is dissolved in 0.1 M $Pb(NO_3)_2$ solution. Furthermore, the c(Pb)/c(Cu) ratios

Table 1 The adsorption experiments using different methods

Sample no.	Method	c(Pb)/c(Cu)[a]
1	Crystalline **1** (10.7 mg) @ $Pb(NO_3)_2$ solution (10 mL, 0.1 M), immersion	1.91×10^{-3}
2	Crystalline **1** (11.1 mg) @ $Pb(NO_3)_2$ solution (10 mL, 0.1 M), mechanically stirred	4.63×10^{-3}
3	Crystalline **1** (10.9 mg) @ $Pb(NO_3)_2$ solution (10 mL, 0.1 M), ultrasonicated	2.01×10^{-2}

[a] The value of c(Pb)/c(Cu) is calculated based on the result of ICP measurements.

in the solid samples of $[Cu(H_2O)(O_3PC_6H_5)]$ are close to those obtained for compound **1** after similar treatments, indicating that the major contribution to the adsorption comes from metal replacement instead of potential adsorption sites on the ligand. Moreover, in both compound **1** and $[Cu(H_2O)(O_3PC_6H_5)]$, the *c*(Pb)/*c*(Cu) ratio after adsorption using method-3 is increased by about one order of magnitude compared with that using method-1, again demonstrating that the exfoliation can significantly enhance the adsorption capability towards Pb ions. The uptake capacity of compound **1** using method-3 is about 12.94 mg g^{-1}, comparable to those found for the carbon nanotubes.[19] As far as we are aware, the adsorption of Pb(II) ions by metal phosphonates has never been documented in the literature thus far.

In summary, a new layered copper organophosphonate $[Cu(H_2O)(2\text{-BTP})]$ (**1**) based on 5-(2-bromothiophenyl)phosphonic acid (2-$BTPH_2$) has been synthesized and characterized. The material can be successfully exfoliated into hybrid nanosheets simply by ultrasonication in an aqueous solution. Interestingly, the exfoliated sample of compound **1** shows a remarkably enhanced adsorption capability toward Pb(II) ions compared with that of the crystalline sample. The results demonstrate a new route to adsorb toxic heavy metal ions in a more efficient way.

This work was financially supported by the National Basic Research Program of China (2010CB923402, 2013CB922100), and the NSF of Jiangsu Province of China (No. BK2009009).

Notes and references

§ Crystal data for **1**: Monoclinic, $P2_1/c$, a = 15.899(4), b = 7.627(2), c = 7.344(2) Å, β = 100.075(4)°, V = 876.7(4) $Å^3$, Z = 4, $F(000)$ = 620, ρ_{calcd} = 2.444 g cm^{-3}, $\mu(MoK_\alpha)$ = 7.44 mm^{-1} (λ = 0.71073 Å), R_1 = 0.0566, wR_2 = 0.1499, GooF = 0.994. CCDC 998012.

1 (*a*) J. Sakamoto, J. van Heijst, O. Lukin and A. D. Schluter, *Angew. Chem., Int. Ed.*, 2009, **48**, 1030; (*b*) J. V. Barth, G. Costantini and K. Kern, *Nature*, 2005, **437**, 671; (*c*) R. Madueno, M. T. Raisanen, C. Silien and M. Buck, *Nature*, 2008, **454**, 618; (*d*) U. Schlickum, R. Decker, F. Klappenberger, G. Zoppellaro, S. Klyatskaya, M. Ruben, I. Silanes, A. Arnau, K. Kern, H. Brune and J. V. Barth, *Nano Lett.*, 2007, **7**, 3813.

2 (*a*) Y. Omomo, T. Sasaki, L. Wang and M. Watanabe, *J. Am. Chem. Soc.*, 2003, **125**, 3568; (*b*) X.-P. Dong, J. Fu and F.-N. Xi, *J. Mater. Res.*, 2011, **26**, 1285; (*c*) C. Zhao, J. Fu, Z. Zhang and E. Xie, *RSC Adv.*, 2013, **3**, 4018.

3 (*a*) Z. Liu, R. Ma, M. Osada, N. Iyi, Y. Ebina, K. Takada and T. Sasaki, *J. Am. Chem. Soc.*, 2006, **128**, 4872; (*b*) R. Z. Ma, J. B. Liang, K. Takada and T. Sasaki, *J. Am. Chem. Soc.*, 2011, **133**, 613; (*c*) G. Li, X. Wang, H. Ding and T. Zhang, *RSC Adv.*, 2012, **2**, 13018.

4 (*a*) S.-H. Yu and M. Yoshimura, *Adv. Mater.*, 2002, **14**, 296; (*b*) J.-w. Seo, J.-t. Jang, S.-w. Park, C. Kim, B. Park and J. Cheon, *Adv. Mater.*, 2008, **20**, 4269; (*c*) M. Chhowalla, H. S. Shin, G. Eda, L. J. Li, K. P. Loh and H. Zhang, *Nat. Chem.*, 2013, **5**, 263.

5 (*a*) V. Eswaraiah, S. S. J. Aravind and S. Ramaprabhu, *J. Mater. Chem.*, 2011, **21**, 6800; (*b*) Q. Zhou, Z. B. Zhao, Y.-S. Chen, H. Hu and J.-S. Qiu, *J. Mater. Chem.*, 2012, **22**, 6061; (*c*) L. Xu, Y. J. Huang, J.-J. Li, D.-L. Wang, M.-M. Chen, J.-J. Tao, K.-P. Cui, G.-Q. Pan, N.-D. Huang and L.-B. Li, *Langmuir*, 2013, **29**, 3813.

6 (*a*) D. M. Kaschak, S. A. Johnson, D. E. Hooks, H.-N. Kim, M. D. Ward and T. E. Mallouk, *J. Am. Chem. Soc.*, 1998, **120**, 10887; (*b*) K. Varoon, X. Y. Zhang, B. Elyassi, D. D. Brewer, M. Gettel, S. Kumar, J. A. Lee, S. Maheshwari, A. Mittal, C. Y. Sung, M. Cococcioni, L. F. Francis, A. V. McCormick, K. A. Mkhoyan and M. Tsapatsis, *Science*, 2011, **334**, 72; (*c*) P. A. Hu, Z. Z. Wen, L. F. Wang, P. H. Tan and K. Xiao, *ACS Nano*, 2012, **6**, 5988; (*d*) M. Naguib, O. Mashtalir, J. Carle, V. Presser, J. Lu, L. Hultman, Y. Gogotsi and M. W. Barsoum, *ACS Nano*, 2012, **6**, 1322; (*e*) F. Saleem, Z.-C. Zhang, B. Xu, X.-B. Xu, P.-L. He and X. Wang, *J. Am. Chem. Soc.*, 2013, **135**, 18304.

7 (*a*) X. Huang and J. Li, *J. Am. Chem. Soc.*, 2007, **129**, 3157; (*b*) T. Yamamoto, N. Saso, Y. Umemura and Y. Einaga, *J. Am. Chem. Soc.*, 2009, **131**, 13196.

8 (*a*) R. Makiura and O. Konovalov, *Dalton Trans.*, 2013, **42**, 15931; (*b*) X.-D. Zhang, Q.-H. Liu, L.-J. Meng, H. Wang, W.-T. Bi, Y.-H. Peng, T. Yao, S.-Q. Wei and Y. Xie, *ACS Nano*, 2013, **7**, 1682.

9 (*a*) R. B. Nielsen, K. O. Kongshaug and H. Fjellvag, *J. Mater. Chem.*, 2008, **18**, 1002; (*b*) P. Amo-Ochoa, L. Welte, R. Gonzalez-Prieto, P. J. S. Miguel, C. J. Gomez-Garcia, E. Mateo-Marti, S. Delgado, J. Gomez-Herrero and F. Zamora, *Chem. Commun.*, 2010, **46**, 3262.

10 (*a*) P.-Z. Li, Y. Maeda and Q. Xu, *Chem. Commun.*, 2011, **47**, 8436; (*b*) J.-C. Tan, P. J. Saines, E. G. Bithell and A. K. Cheetham, *ACS Nano*, 2012, **6**, 615; (*c*) P. J. Saines, J.-C. Tan, H. H. M. Yeung, P. T. Barton and A. K. Cheetham, *Dalton Trans.*, 2012, **41**, 8585.

11 (*a*) P. O. Adelani and T. E. Albrecht-Schmitt, *Angew. Chem., Int. Ed.*, 2010, **49**, 8909; (*b*) M. Plabst, L. B. McCusker and T. Bein, *J. Am. Chem. Soc.*, 2009, **131**, 18112; (*c*) M. T. Wharmby, J. P. S. Mowat, S. P. Thompson and P. A. Wright, *J. Am. Chem. Soc.*, 2011, **133**, 1266.

12 (*a*) O. R. Evans, H. L. Ngo and W. Lin, *J. Am. Chem. Soc.*, 2001, **123**, 10395; (*b*) L. Ma, C. Abney and W. Lin, *Chem. Soc. Rev.*, 2009, **38**, 1248.

13 (*a*) X. Liang, F. Zhang, W. Feng, X. Zou, C. Zhao, H. Na, C. Liu, F. Sun and G. Zhu, *Chem. Sci.*, 2013, **4**, 983; (*b*) J. M. Taylor, R. K. Mah, I. L. Moudrakovski, C. I. Ratcliffe, R. Vaidhyanathan and G. K. H. Shimizu, *J. Am. Chem. Soc.*, 2010, **132**, 14055.

14 (*a*) S.-S. Bao, Y. Liao, Y.-H. Su, X. Liang, F.-C. Hu, Z.-H. Sun, L.-M. Zheng, S.-Q. Wei, R. Alberto, Y.-Z. Li and J. Ma, *Angew. Chem., Int. Ed.*, 2011, **50**, 5504; (*b*) Y.-Z. Zheng, M. Evangelisti, F. Tuna and R. E. P. Winpenny, *J. Am. Chem. Soc.*, 2011, **134**, 1057; (*c*) P.-F. Wang, Y. Duan, J. M. Clemente-Juan, Y. Song, K. Qian, S. Gao and L.-M. Zheng, *Chem. – Eur. J.*, 2011, **17**, 3579.

15 T. Araki, A. Kondo and K. Maeda, *Chem. Commun.*, 2013, **49**, 552.

16 Elemental anal. calcd for $[Cu(BrC_4H_2SPO_3)]$ (**2**): C, 15.76; H, 0.65. Found: C, 15.75; H, 1.31. IR (KBr, cm^{-1}): 3441m, 1633w, 1501w, 1408s, 1301w, 1209w, 1099s, 1072s, 1050s, 1007s, 965s, 944s, 800m, 740w, 668m, 586s, 543w, 451m.

17 O. Kahn, *Molecular Magnetism*, VCH Publishers, Inc., New York, 1993.

18 H.-C. Yao, Y.-Z. Li, S. Gao, Y. Song, L.-M. Zheng and X.-Q. Xin, *J. Solid State Chem.*, 2004, **177**, 4557.

19 Y. H. Li, Y. Zhu, Y. Zhao, D. Wu and Z. Luan, *Diamond Relat. Mater.*, 2006, **15**, 90.

20 Y. P. Zhang and A. Clearfield, *Inorg. Chem.*, 1992, **31**, 2821.